

NANO LETTERS

Analysis of Optical Absorption in Silicon Nanowire Arrays for Photovoltaic Applications

Lu Hu and Gang Chen*

Massachusetts Institute of Technology, Cambridge, Massachusetts 02139

Received April 30, 2007; Revised Manuscript Received August 20, 2007

ABSTRACT

This paper presents analysis of the optical absorption in silicon nanowire arrays that have potential applications in solar cells. The effects of wire diameter, length, and filling ratio on the absorptance of nanowire arrays are simulated. The study reveals that nanowire arrays with moderate filling ratio have much lower reflectance compared to thin films. In a high-frequency regime, nanowire arrays have higher absorptance than their thin film counterparts. In low-frequency regime, nanowire arrays absorb less but can be designed to approach that of the film by changing the filling ratio.

Nanowires and nanotubes can serve as electrodes for polymer and electrochemical photovoltaic cells^{1,2} and building blocks in other novel optical devices.^{3,4} Recently photovoltaic cells based on silicon nanowire arrays have been suggested as a promising candidate for solar energy harvesting.⁵ The advantage of the silicon nanowire photovoltaic cell lies in its short collection length for excited carriers, resulting in significant improvement in carrier collection efficiency. The optical absorption characteristics of nanowire arrays in the solar spectrum, one of the key factors that determine the efficiency of solar cells, remain unclear. A detailed analysis of the optical absorption will help the design and optimization processes of the silicon nanowire solar cells. In this letter, we numerically analyze the effects of wire diameter, length, and filling ratio on the optical absorption of periodic nanowire arrays and compare the cases with the results of silicon thin films. We found that, in comparison to thin films,

nanowire array based solar cells have an intrinsic antireflection effect that increases absorption in short wavelength range. Although this paper focuses on silicon nanowire arrays, results obtained are also of interest to other photovoltaic devices using nanowires as electrodes.

Figure 1 shows the schematics of the periodic nanowire structure under study. The direction of the incoming solar radiation is determined by the zenith (θ) and azimuthal (φ) angles. The parameters of the structure are the period a of the square lattice, wire diameter d , and wire length L . We consider two limiting cases for the substrate: air and perfect metal. In our analysis, we consider crystalline silicon nanowires with diameters between 50 and 80 nm, which are readily fabricated by current nanofabrication techniques.^{6,7} For wires with such small diameters, we need to take into account the wave effects by solving the full wave vector Maxwell's equations. The transfer matrix method (TMM) has been proven to be very effective for dealing with such

* Corresponding author. E-mail: gchen2@mit.edu.

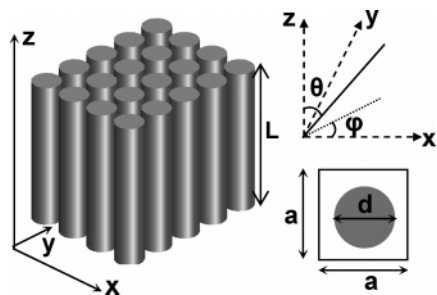


Figure 1. Schematic drawing of the periodic silicon nanowire structure. The parameters are the length L , the period a , and the diameter d . In the figure, θ and φ are the zenith and azimuthal angles, respectively.

periodic structures.^{8,9} The TMM is a finite difference frequency domain method, where the fields on one side of a unit cell are related to those on the end by a transfer matrix. The reflection and transmission matrices of a structure can then be obtained by decomposing the fields into plane wave components. In our calculations, we use a fine grid ($4.5 \text{ nm} \times 4.5 \text{ nm} \times 4.5 \text{ nm}$), which is less than $1/10$ of the shortest wavelength in the whole computation domain, in order to ensure the convergence. By energy balance, the absorbance of the wire structure is given by $A(\omega) = 1 - R(\omega) - T(\omega)$, where ω is the frequency of the incident wave, and R , T , and A are the frequency dependent reflectance, transmittance, and absorbance of the wire structure. The frequency range of interest is from 1.1 to 4 eV, where most of the above-band-gap photons concentrate in silicon-based materials. In this frequency range, the permittivity of silicon shows dispersion. In this paper, we only consider lightly doped silicon.⁵ At frequencies above the band gap, the difference in the optical constants between lightly doped and intrinsic silicon is negligible,¹⁰ which gives us the convenience of using the same optical constants for both p and n regions of the core-shell structure in a silicon nanowire solar cell.⁵ For the calculations, we take the experimentally measured optical constants of intrinsic silicon from ref 11.

Figure 2a shows the optical absorbance of an array of silicon nanowires with a diameter of 50 nm. The incident wave is normal to the x - y plane with the electric field polarized along the x -axis. Three wire lengths, 1.16, 2.33, and $4.66 \mu\text{m}$, are selected to show the thickness-dependent absorption. These lengths are comparable to the film thickness in silicon thin film solar cells.^{12–14} The absorbance of a $2.33 \mu\text{m}$ silicon thin film is also plotted in the same figure as a reference. As seen in the figure, for photons with energy just above the 1.1 eV band gap, the optical absorption is very limited for all wire lengths due to the fact that silicon has an indirect band gap and the optical absorption needs phonon assistance. As the frequency increases, the absorption of nanowires rises and reaches a plateau region shared by all lengths. The absorbance for nanowires in the plateau region is higher than that of the optically denser thin film, while in the low-energy photon regime, the absorption in the film is more efficient.

The total absorption in the nanowire structure is determined by both reflection and transmission. To understand

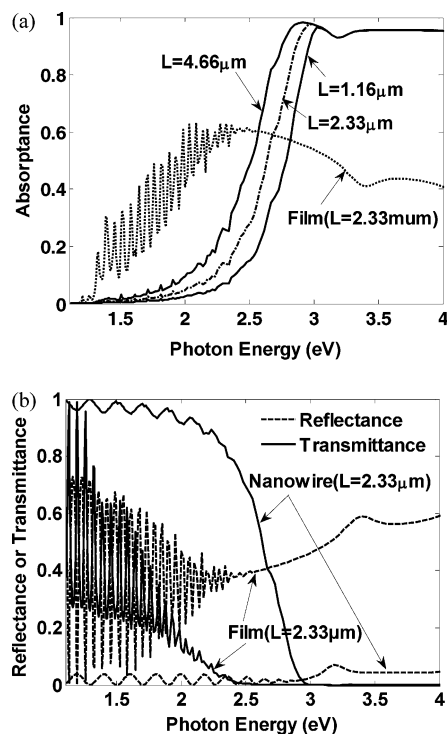


Figure 2. Radiative properties of nanowire structures with various thickness, (a) absorbance of nanowires with $L = 1.16$, 2.33 , and $4.66 \mu\text{m}$ ($d = 50 \text{ nm}$ and $a = 100 \text{ nm}$). The absorbance of a thin film is included as a reference, and (b) reflectance of nanowires and the thin film.

the trend of absorption in nanowire arrays, in Figure 2b, we plot the reflectance and transmittance for a nanowire structure ($d = 50 \text{ nm}$ and $a = 100 \text{ nm}$) and a thin film. Both structures have a thickness of $2.33 \mu\text{m}$. Note that the period of the cell we consider is smaller than the wavelength range of interest such that only the zeroth-order reflection and transmission exist. It can be seen that the reflectance of nanowires is significantly lower than that of the thin film in the entire spectral range due to the reduced density of the nanowire structures. For low frequencies, the extinction coefficient of silicon is small and interference effects exist, resulting in the oscillation of reflectance and transmittance. The interference effect is much stronger in the film than in the nanowire array, again due to the decreased density of the nanowire array. In the high-frequency regime, the absorption increases and the interference effect diminishes around 3 eV. In Figure 2b, the transmittances for the nanowire and the thin film are also presented. In the low-frequency regime, the figure shows that the transmittance of the nanowire structure is higher than the thin film. The higher transmittance cannot be compensated by the low reflectance, leading to insufficient absorption of low-energy photons in the nanowire structure.

It is interesting to note that such small reflection in the entire spectrum can only be achieved in the thin film solar cell by applying special antireflection coatings.^{14–16} It is the combined effect of small reflection and zero transmittance in the high-frequency regime that causes higher absorption in nanowires than their thin film counterparts. It may appear surprising that, in the high-frequency regime, the transmittance of the nanowires is zero, considering the structure is

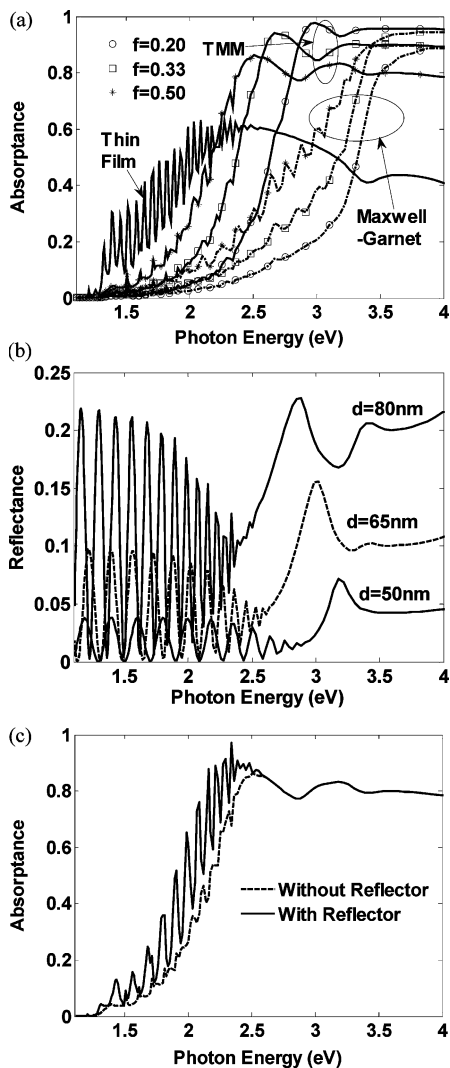


Figure 3. Radiative properties of nanowire structures with various filling ratios, (a) absorbance obtained by TMM and Maxwell-Garnet approximation, (b) reflectance of nanowires with diameter of 50, 65, and 80 nm, and (c) absorbance of nanowires with and without a back reflector ($d = 80$ nm).

“porous”. In fact, when the diameter of the nanowire is comparable to or smaller than the wavelengths of incident solar light, the geometric-optics definition of incident area does not apply. A nanowire can actually absorb not only the portion of a wave incident directly on it but also the surrounding wave. It is well-known that a small single particle can have larger absorption cross section than its geometric cross section.¹⁷ The total absorption of the incident wave in nanowires is another example of this small size effect in a clustered structure. However, despite the superior optical absorption ability in the high-frequency regime, the extinction coefficient of silicon is too small to absorb the long wavelength solar radiation. Increasing the length of nanowires is needed to enhance the absorption, as shown in Figure 2a, where the absorption in the low-frequency regime is improved by using longer nanowires.

The absorbance of nanowire structures with different filling ratios is shown in Figure 3a. The incident wave is normal to the x – y plane, with the electric field polarized along the x -axis. All structures have a fixed period of

100 nm and wire length of $2.33 \mu\text{m}$, but the wire diameter varies. As a reference, the absorbance of a silicon thin film ($2.33 \mu\text{m}$ in thickness) is presented in the same figure. For comparison, the absorbance based on the Maxwell-Garnett effective medium approximation¹⁸ is also plotted in the same figure. Maxwell-Garnett approximation generally follows the trend given by the TMM results but does not agree very well with the exact numerical solutions. This discrepancy is expected because Maxwell-Garnett theory is based on the assumption that the dielectric inclusion is dilute, while in closely packed nanowire structures, the electromagnetic interaction between nanowires cannot be neglected. Figure 3b shows the reflectance of the nanowire structures, where smaller filling ratios yield less reflection consistently. However, as seen in the figure, larger filling ratios give higher absorption in the low-frequency regime for the same wire length, while in the high-frequency regime, nanowires with smaller filling ratios absorb more light. To evaluate the overall absorption performance of the nanowire structures in the solar spectrum, we calculated the ultimate efficiency¹⁹ using the Air Mass 1.5 direct normal and circumsolar spectrum:²⁰

$$\eta = \frac{\int_{\nu_g}^{\infty} \frac{I_{\nu} \nu_g}{\nu} d\nu}{\int_0^{\infty} I_{\nu} d\nu} \quad (1)$$

where ν is the photon frequency, I_{ν} the spectral solar intensity, and ν_g is the frequency corresponding to the silicon band gap. Equation 1 assumes each photon with energy greater than the band gap produces only one electron–hole pair with energy equal to $h\nu_g$, with the excessive energy converted to heat. The absorption efficiencies are 5.80%, 9.47%, 12.50%, and 15.50% for the 50, 65, and 80 nm nanowires and the thin film, respectively. The calculations show that, by changing filling ratios, a nanowire structure can have overall absorption efficiency close to its thin film counterpart. Furthermore, the long wavelength absorption in nanowire structures can be improved to some extent by employing light trapping to increase the optical path.^{21,22} As a proof of concept, we show in Figure 3c that by putting a perfect reflecting mirror (100% reflectivity) on the backside of the 80 nm nanowire structure, the overall absorbance efficiency is enhanced from 12.50% to 16.09% due to the enhancement in the long wavelength (low frequency) regime.

We have considered normal incidence ($\theta = 0^\circ$) with the electric field polarized along the x -axis ($\varphi = 0^\circ$) heretofore. Figure 4 shows the absorbance of a nanowire structure (no back reflector) with $a = 100$ nm, $d = 80$ nm, and $L = 2.33 \mu\text{m}$ for nonzero θ and φ angles. As shown in the figure, the difference between TE polarized light with $(\theta, \varphi) = (0^\circ, 0^\circ)$, $(0^\circ, 20^\circ)$, and $(0^\circ, 40^\circ)$ are negligible, suggesting that for the wavelengths of interest the nanowire structure is almost isotropic in the x – y plane. When the incidence is oblique ($(\theta, \varphi) = (30^\circ, 0^\circ)$), TE polarization has lower absorption than TM polarization because the latter has an electric field component along the wire axis which facilitates the absorption.

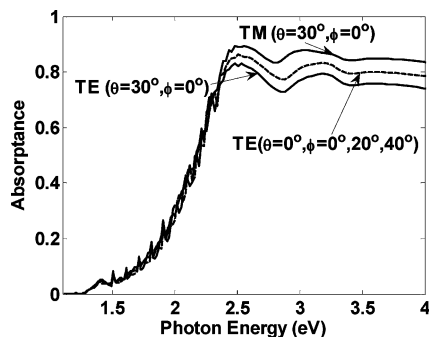


Figure 4. Angular dependence of absorbance for a nanowire structure with $d = 80$ nm, $a = 100$ nm, and $L = 2.33$ μ m. The absorbance curves of $\varphi = 0^\circ$, 20° , and 40° are overlapped.

In summary, we have studied the optical absorption in periodic nanowire structures for photovoltaic applications. Our calculation shows that the electromagnetic interaction between nanowires cannot be neglected which invalidates the Maxwell-Garnett approach. Compared to thin films, the nanowire structures have the advantage of small reflection in a wide spectrum range, which can be achieved without specially designed antireflection coatings. The small reflection from the nanowire structures improves the optical absorption significantly in the high-frequency regime, whereas in the low-frequency regime, the improvement cannot be achieved due to the small extinction coefficient of silicon. The less ideal absorption in the low-frequency regime can be overcome by applying light-trapping techniques or using longer wires.

Acknowledgment. We thank Dr. Xiaoyuan Chen for helpful comments, and DOE and NSF for partial financial support.

References

- (1) Huynh, W. U.; Dittmer, J. J.; Alivisatos, A. P. *Science* **2002**, 295, 2425.
- (2) Law, M.; Greene, L. E.; Johnson, J. C.; Saykally, R.; Yang, P. *Nat. Mater.* **2005**, 4, 455.
- (3) Wang, Y.; Kempa, K.; Kimball, B.; Carlson, J. B.; Benham, G.; Li, W. Z.; Kempa, T.; Rybczynski, J.; Herczynski, A.; Ren, Z. F. *Appl. Phys. Lett.* **2004**, 85, 2607.
- (4) Rybczynski, J.; Kempa, K.; Wang, Y.; Ren, Z. F.; Carlson, J. B.; Kimball, B. R.; Benham, G. *Appl. Phys. Lett.* **2006**, 88, 203122.
- (5) Kayes, B. M.; Atwater, H. A.; Lewis, N. S. *J. Appl. Phys.* **2005**, 97, 114302.
- (6) Lauhon, L. J.; Gudiksen, M. S.; Wang, D.; Lieber, C. M. *Nature* **2002**, 420, 57.
- (7) Law, M.; Goldberger, J.; Yang, P. *Annu. Rev. Mater. Res.* **2004**, 34, 83.
- (8) Pendry, J. B. *J. Mod. Optic.* **1994**, 41, 209.
- (9) Bell, P. M.; Pendry, J. B.; Moreno, L. M.; Ward, A. J. *Comput. Phys. Commun.* **1995**, 85, 306.
- (10) Jellison, G. E., Jr.; Modine, F. A.; White, C. W.; Wood, R. F.; Young, R. T. *Phys. Rev. Lett.* **1981**, 46, 1414.
- (11) *Handbook of Optical Constants of Solids*; Palik, E. D., Ed.; Academic: Orlando, FL, 1985.
- (12) Brendel, R.; Bergmann, R.; Lolgen, P.; Wolf, M.; Werner, J. *Appl. Phys. Lett.* **1997**, 70, 390.
- (13) Yamamoto, K. *IEEE Trans. Electron. Devices* **1999**, 46, 2041.
- (14) Yamamoto, K.; Nakajima, A. A.; Yoshimi, M.; Sawada, T.; Fukuda, S.; Suezaki, T.; Ichikawa, M.; Koi, Y.; Goto, M.; Meguro, T.; Matsuda, T.; Kondo, M.; Sasaki, T.; Tawada, Y. *Sol. Energy* **2004**, 77, 939.
- (15) Rowlands, S. F.; Livingstone, J.; Lund, C. P. *Sol. Energy* **2004**, 76, 301.
- (16) Koynov, S.; Brandt, M. S.; Stutzmann, M. *Appl. Phys. Lett.* **2006**, 88, 203107.
- (17) Kattawar, G. W.; Eisner, M. *Appl. Opt.* **1970**, 9, 2685.
- (18) Maxwell-Garnett, J. C. *Philos. Trans. R. Soc. London* **1904**, 203, 385.
- (19) Shockley, W.; Queisser, H. J. *J. Appl. Phys.* **1961**, 32, 510.
- (20) Air Mass 1.5 Spectra, American Society for Testing and Materials, <http://rredc.nrel.gov/solar/spectra/am1.5/>.
- (21) Green, M. A. *Prog. Photovoltaics: Res. Appl.* **1999**, 7, 317.
- (22) Krc, J.; Zeman, M.; Smole, F.; Topic, M. *Thin Solid Films* **2004**, 451–452, 298.

NL071018B